Synthesis and spectroelectrochemical investigation of two tetraarylporphyrins

Robin A. Krüger, Andrea S. Terpstra, and Todd C. Sutherland

Abstract: A free-base tetraarylporphyrin was synthesized by the [2+2] macrocyclization of a dipyrromethane derivative with 3,4,5-tris(dodecyloxy)benzaldehyde in 61% yield. The free-base porphyrin was metallated with zinc acetate in 94% conversion. The free-base and metallated porphyrins show typical intense Soret bands at 426 and 425 nm, respectively, along with the expected number and intensity of Q-bands. Both porphyrins are also fluorescent and display small Stokes shifts between 13 and 18 nm. Cyclic voltammetry established that each porphyrin underwent two reversible one-electron oxidations at 492 and 725 mV (vs Fc/Fc^+ (ferrocene reference)) for the free-base porphyrin and at 329 and 589 mV (vs Fc/Fc^+) for the Zn-metalloporphyrin. Electron-transfer rates were also determined to fall between 1.2×10^{-3} and 2.4×10^{-3} cm s^{-1}. In addition, spectroelectrochemistry and density functional theory calculations of the oxidized products were carried out to confirm the macrocyclic ring oxidations.

Key words: porphyrinoids, electrochemistry, redox chemistry, photochemistry, density functional calculations.

Résumé : On a réalisé la synthèse d'une tétraaraylporphyrine sous la forme de base libre avec un rendement de 61 % par macrocyclisation [2+2] d'un dérivé de dipyrrométhane avec du 3,4,5-tris(docécyloxo)benzaldéhyde. On a effectué la métallation de la porphyrine à l'état de base libre, avec un rendement de 94 %, par traitement avec de l'acétate de zinc. La base libre et la porphyrine métallée présentent respectivement les bandes typiques intenses de Soret à 426 et à 425 nm ainsi que le nombre et l'intensité attendu des bandes Q. Les deux porphyrines sont aussi fluorescentes et elles présentent de faibles déplacements de Stokes, entre 13 et 18 nm. La voltampérométrie cyclique a permis d'établir que chaque porphyrine subit deux oxydations réversibles à un électron, à 492 et 725 mV (vs Fc/Fc^+) pour la base libre et à 329 et 589 mV (vs Fc/Fc^+) pour la Zn-métalloporphyrine. On a aussi déterminé que les vitesses de transfert d'électron se situent entre $1,2 \times 10^{-3}$ et $2,4 \times 10^{-3}$ cm s^{-1}. De plus, de la spectroélectrochimie et des calculs d'après la théorie de la fonctionnelle de la densité effectués sur les produits oxydés pour confirmer les oxydations des noyaux macrocycliques.

Mots-clés : porphyrinoïdes, électrochimie, chimie d'oxydoréduction, photochimie, calculs de la fonctionnelle de la densité.

[Traduit par la Rédaction]

Introduction

Porphyrinoids are commonly found compounds in both the animal and plant kingdoms, as they play important roles in the key steps of photosynthesis that ultimately convert sunlight into chemical energy.[1,2] Iron porphyrins play critical roles in oxygen transport,[3,4] peroxide reduction,[5–7] drug metabolism (cytochrome P450),[8,9] and the mitochondrial electron-transport chain.[10,11] Because of their prevalence in nature, exploration of their potential applications in organic materials is warranted. Photoinitiated charge-transfer reactions are key steps in solar energy conversion,[2,12,13] device applications,[14] and catalysis.[15,16] Progress in these applications necessitates a critical understanding of the thermodynamic factors that direct the charge-transfer reactions. Excited-state reactants are versatile intermediates because they are both better electron donors and better electron acceptors than their ground-state counterparts.[17–19] The reducing and oxidizing strength of these excited-state reagents is crucial to understanding the driving forces that are operating in the eventual applications. Generally, porphyrin ring systems can be easily oxidized to radical cations and sometimes dications.[20–24] Importantly, these cations are stable at room temperature and can be used as reactive intermediates that could be used in organic materials applications.

This contribution explores the electronic properties of two porphyrins and compares them with two well-characterized porphyrins, namely free-base tetraphenylporphyrin (TPP) and Zn-TPP. In addition, full electrochemical and density functional theory (DFT) studies were carried out to assess the charge-transport properties of the oxidized porphyrin ring systems. The goal of this work is to install electron-rich substituents to the meso positions of porphyrins to make stabilized cations for use as light-harvesting chromophores in solar cell applications. Important parameters for a candidate material are high molar absorptivity and excited-

Received 26 February 2010. Accepted 20 May 2010. Published on the NRC Research Press Web site at canjchem.nrc.ca on 25 January 2011.

This article is part of a Special Issue dedicated to Professor J. C. Scaiano.

R.A. Krüger, A.S. Terpstra, and T.C. Sutherland.[1] Department of Chemistry, University of Calgary, 2500 University Drive NW, Calgary, AB T2N 1N4, Canada.

[1] Corresponding author (e-mail: todd.sutherland@ucalgary.ca).

doi:10.1139/V10-098

state redox potential that are compatible with a typical *n*-type material, such as phenyl-C_{61}-butyric acid methyl ester (PCBM), and ground-state stability of the radical cation. Furthermore, these compounds were synthesized to explore whether supramolecular structures, such as liquid crystals, could form using meso-aryl substituted porphyrins. A common motif, the trisalkoxyphenyl group, has been employed in a variety of functional materials[25–29] to impart supramolecular long-range ordering that may enhance charge transport in solar applications.

Experimental

Zinc-porphyrin (4)

Free-base porphyrin (30 mg, 10.6 μmol), $NaHCO_3$ (100 mg, 450 μmol) and zinc acetate dihydrate (100 mg, 450 mmol) were stirred at ambient temperature in $CHCl_3$ for 4 h in the dark. The red solution was then poured on diluted aqueous $NaHCO_3$ solution (50 mL). After phase separation, the aqueous layer was extracted with CH_2Cl_2 (1 × 20 mL) and the combined organic layers were dried with $MgSO_4$ and evaporated. The crude red oil was purified by column chromatography using CH_2Cl_2 as the eluent on alumina (N, III) and collection of the first red fraction. The yield was 29 mg (10 μmol, 94%). ^1H NMR (CD_2Cl_2, 400 MHz) δ: 9.10 (s, 8 H, aryl-H), 7.45 (s, 8 H, pyr-H), 4.29 (t, *J* = 6.6 Hz, 8 H, OCH_2), 4.11 (t, *J* = 6.5 Hz, 16 H, OCH_2), 2.01–1.94 (m, 8 H, CH_2), 1.93–1.86 (m, 16 H, CH_2), 1.72–1.65 (m, 8 H, CH_2), 1.56–1.25 (m, 208 H, CH_2), 0.93 (t, *J* = 7.0 Hz, 12 H, CH_3), 0.87 (t, *J* = 7.0 Hz, 24 H, CH_3). UV–vis (CH_2Cl_2) λ_{abs} (nm) [ε (L mol^{-1} cm^{-1})] = 425 [130 000], 550 [6600], 589 [1300]. λ_{em} (nm) (relative intensity) (λ_{ex} = 425 nm) = 607 (0.96), 649 (1). HR–MS (MALDI-TOF) calcd. for $C_{188}H_{316}N_4O_{12}Zn$: 2886.353; found: 2886.365.

Results and discussion

The synthesis of metal-free porphyrin **3** and Zn-porphyrin **4** is shown in Scheme 1. The synthesis of **1** was carried out using literature methods.[30,31] Condensation of freshly distilled excess pyrrole and TFA with **1** resulted in the formation of the dipyrromethane **2** in 57% yield. Note that **2** was moderately stable at room temperature under N_2 atmosphere and was immediately used in the ring-closing condensation with **1** to produce the free-base porphyrin **3** in 61% yield.[32] Porphyrin **3** was easily metallated with Zn-acetate at room temperature in the dark to give Zn-porphyrin **4** in 94% yield. The electronic absorption and emission properties of porphyrins **3** and **4** are summarized in Table 1, and the spectra are included in the Supplementary data. Both **3** and **4** exhibit strong near-UV absorptions (Soret) attributed to the $S_0 \rightarrow S_2$ transition and sets of weaker visible transitions (Q-bands) attributed to the $S_0 \rightarrow S_1$ transitions, typical of porphyrins.[33] The absorption and emission properties of **3** and **4** are consistent with other reports, which have been extensively reviewed.[34]

The Soret peak, B(0,0), for **3** is positioned at 426 nm with a full width at half maximum (FWHM) of 20 nm, which is similar to the Soret band of **4** at 425 nm with a narrower FWHM of 14 nm (see Supplementary data). The Soret bands of **3** and **4** are slightly red-shifted compared with Soret bands of free-base tetraphenylporphyrin (H_2-TPP) and Zn-tetraphenylporphyrin (Zn-TPP) because of the electron-donating tris(alkoxy) meso-substituents.

Scheme 1. Synthesis of Zn-porphyrin.

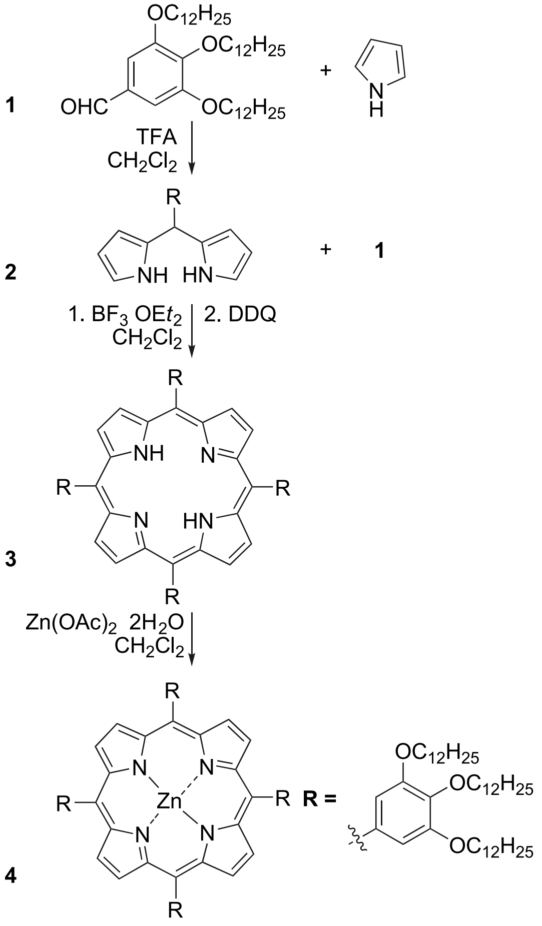

The emission spectra of **3** and **4** are similar to the emission spectra of H_2-TPP and Zn-TPP, respectively. Note the excitation wavelength used in each compound was the peak of the Soret band. Free-base porphyrin **3** has two emission peaks at 661 nm and 722 nm with peak height ratios of 1 to 0.44. The Q(0,0) peak position of **3** is red-shifted by 11 nm compared with H_2-TPP, whereas the vibronic sideband of **3** is red-shifted by only 5 nm, accompanied by a ~50% decrease in peak intensity compared with H_2-TPP. The emission spectrum of Zn-porphyrin **4** also exhibits two red-shifted peaks compared with Zn-TPP at 607 nm and 649 nm. The emission peaks are typical for porphyrinoid compounds and are consistent with emission from singlet excited states. Triplet emissions typically show at 800 nm and greater wavelengths.

Charge-transfer dynamics were assessed by cyclic voltammetry (CV) for the oxidation reaction. Figure 1*a* shows the cyclic voltammagrams of **3** at various scan rates. Each voltammagram shows two quasi-reversible oxidation waves, which are assigned to two, one-electron oxidation steps, consistent with other reports of related porphyrins.[35–40] The half-wave potentials ($E_{1/2}^{ox}$) were calculated from the average of the anodic and cathodic peaks of each step, which results

Table 1. Absorption and luminescence peaks of **3** and **4** in CH_2Cl_2 at room temperature.

	Absorption peaks[a]				Luminescence peaks[b]			
	B(0,0)	Q_y(1,0)	Q_y(0,0)	Q_x(1,0)	Q_x(0,0)	Q(0,0)	Q(0,1)	Stokes shift (nm)
H_2-TPP[c]	419(413)	514(19.4)	547(8.2)	592(6.6)	646(4.6)	650(1)	717(0.84)	4
3	426(151)	518(7.1)	555(3.4)	592(2.2)	648(1.7)	661(1)	722(0.44)	13
Zn-TPP[c]	422(574)			548(29.9)	588(5.1)	595(1)	645(2.1)	7
4	425(130)			550(6.6)	589(1.3)	607(1)	649(1.1)	18

Note: H_2-TPP, free-base tetraphenylporphyrin; Zn-TPP, zinc-tetraphenylporphyrin.

[a] All absorption peaks are shown in nanometres followed by molar absorptivities in parentheses with units of 10^3 L mol^{-1} cm^{-1}.

[b] All luminescence peaks are shown in nanometres followed by ratio of intensities. Compounds were excited at B bands.

[c] These data were taken from PhotoChemCAD.

in $E_{1/2}^{ox}(1)$ of 492 mV and $E_{1/2}^{ox}(2)$ of 725 mV vs Fc/Fc^+ (ferrocene reference). The difference between the two oxidation half-wave potentials is 233 mV, which is similar to H_2-TPP.

The CV at slow scan rate (20 mV s^{-1}) provides a good indication of reversibility with peak separations of 78 mV between anodic and cathodic redox couples, where peak separations of 57 mV are considered ideal reversible Nernstian behaviour. The capacitive current, which is quantified as the difference between anodic and cathodic currents in a region that does not contain Faradic responses, is unexpectedly large. There are reports of alkyl-derivatized porphyrins that form liquid crystals[41–44] or films on electrodes[45–48] and this is possible with compound **3**; however, porphyrin **3** is very soluble in CH_2Cl_2, which should minimize film formation. In addition, the linear plot in Fig. 1*b* indicates the redox reaction is diffusion controlled. Peak current is related to scan rate according to eq. [1][49]

$$[1] \qquad i_p = (2.69 \times 10^5) n^{3/2} A D_O^{1/2} C_O^* \upsilon^{1/2}$$

where i_p is the peak current in amperes, n is the number of electrons involved in the redox reaction, A is the area of the electrode surface in cm^2, D_O is the diffusion constant of the oxidized species in cm^2 s^{-1}, C_O is the concentration of redox species in mol cm^{-3}, and ν is the scan rate in V s^{-1}. From eq. [1], plots in Fig. 1*b* can be used to determine the diffusion coefficient, assuming the diffusion coefficients of the oxidized and reduced porphyrins are equal ($D_O \approx D_R$). The diffusion coefficients for $\mathbf{3}^+$ and $\mathbf{3}^{2+}$ were found to be 3.3×10^{-7} cm^2 s^{-1} and 5.6×10^{-7} cm^2 s^{-1}, respectively. Using the Stokes–Einstein equation and assuming spherical compounds, these diffusion coefficients correspond to radii of 16 nm and 9 nm for $\mathbf{3}^+$ and $\mathbf{3}^{2+}$, respectively. Clearly, these hydration radii are much larger than the molecular dimensions and could indicate aggregates are forming in solution under CV conditions that are not present at the concentrations used for optical studies. The proposal of aggregate formation is also consistent with the large non-Faradic currents and broad peaks due to different sizes of aggregates. The estimate of the diffusion coefficient enables the use of Nicholson's approach[50] to calculating the electron-transfer rate constant from the difference in peak potentials at each scan rate. The standard rate constants (k_0) for the first and second one-electron oxidations, shown in eq. [2], are 2.4×10^{-3} cm s^{-1} and 1.4×10^{-3} cm s^{-1}, respectively, for **3**. The electron-transfer rate constants for **3** are typical for numerous porphyrin systems.[51]

Fig. 1. (*a*) Cyclic voltammagram of **3** (4.5×10^{-4} mol L^{-1}) in CH_2Cl_2 containing 0.1 mol L^{-1} tetrabutylammonium hexafluorophosphate ($TBAPF_6$) at various scan rates using a glassy carbon electrode, a Ag|AgCl|KCl3M reference electrode, and a Pt wire counter electrode at 25 °C. (*b*) Peak heights of the two oxidation and reduction peaks as a function of the square root of the scan rate for porphyrin **3**.

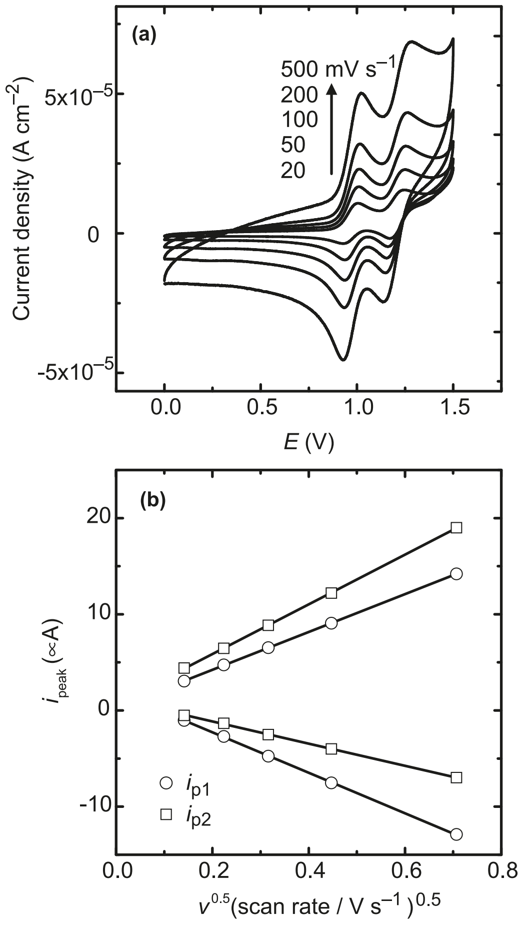

$$[2] \qquad \mathbf{3} \xrightarrow[k_0^1]{-e^-} \mathbf{3}^+ \xrightarrow[k_0^2]{-e^-} \mathbf{3}^{2+}$$

The CVs at increasing scan rates of Zn-porphyrin **4** are included in the Supplementary data because they are similar to those of the free-base porphyrin **3**, exhibiting two quasi-reversible, one-electron oxidation steps. The two redox waves are typical for several Zn-porphyrinoid compounds[52]

Table 2. Summary of electrochemical parameters.

Compound	$E^{ox}_{1/2}(1)$ (mV)	$E^{ox}_{1/2}(2)$ (mV)	ΔE (mV)	$D_O(1)$ (10^{-6} cm^2 s^{-1})	$D_O(2)$ (10^{-6} cm^2 s^{-1})	$k_0(1)$ (10^{-3} cm s^{-1})	$k_0(2)$ (10^{-3} cm s^{-1})	$r_H(1)$ (nm)	$r_H(2)$ (nm)
3	492	725	233	0.33	0.56	2.4	1.4	16	9
4	329	589	260	1.4	2.8	1.2	1.9	4	2

Note: All potentials are referenced to Fc/Fc$^+$. Diffusion coefficients of oxidized and reduced species were assumed to be the same. Rate constants were calculated using Nicholson's method. Hydration radii were calculated using solvent viscosity of CH_2Cl_2 at 0.413 mPa s.

and the peaks are also easier to oxidize than **3**. The two half-wave potentials of **4**, $E^{ox}_{1/2}(1)$ and $E^{ox}_{1/2}(2)$, were 329 mV and 589 mV vs Fc/Fc$^+$, respectively. The difference between the two oxidation half-wave potentials is 260 mV, which is similar to the difference in the case of Zn-TPP. The peak separation at the slowest scan rate (10 mV s^{-1}) is 88 mV and 81 mV for the first and second oxidation peaks, respectively, consistent with quasi-reversible redox reactions.

The capacitive currents in Zn-porphyrin **4** are much less than in the CVs for free-base porphyrin **3**, even though the concentration of **4** in the electrochemical cell was higher than that of **3**. In comparing the CVs of **3** and **4**, it is clear that the CV of **3** displays unique diffusion effects. Employing eq. [1], the diffusion coefficients were calculated to be 1.4×10^{-6} cm^2 s^{-1} and 2.8×10^{-6} cm^2 s^{-1} for **4**$^+$ and **4**$^{2+}$, respectively, resulting in hydration radii of 4 nm and 2 nm for **4**$^+$ and **4**$^{2+}$, respectively. Although the diffusion coefficients are much higher in the Zn-porphyrin case, the standard electron-transfer rates constants for the first and second oxidation reactions are 1.2×10^{-3} cm s^{-1} and 1.9×10^{-3} cm s^{-1}, respectively, which are similar to those of compound **3**. A summary of all electrochemical results is included in Table 2.

The electrochemical oxidation potentials in conjunction with the highest-energy fluorescent band, corresponding to the lowest-lying singlet state, allow for the estimation of the excited-state oxidation potential, first described by Rehm and Weller[53,54] in eq. [3].

$$[3] \qquad E^{*ox}_{1/2} = E^{ox}_{1/2} - E_{00} + \omega_r$$

where $E^{*ox}_{1/2}$ is the excited-state oxidation potential, $E^{ox}_{1/2}$ is the ground-state redox potential, E_{00} is the energy gap between the zeroth vibrational levels of the ground and excited states, and ω_r is the electrostatic work term. For this work, it is assumed that the electrostatic work term has been adequately accounted for within the measurement of the ground-state redox potentials. The excited-state oxidation potentials for **3** and **4** are –1.39 V and –1.71 V vs Fc/Fc$^+$, respectively. For comparison, H_2-TPP is estimated to have a singlet excited-state redox potential of –1.32 V vs Fc/Fc$^+$.[55] The second oxidation potential was not calculated because the fluorescence spectrum of the radical cation is unknown.

The absorption spectrum of **3** oxidized to **3**$^+$ is shown in Fig. 2*a*. Figure 2*a* shows three main features consistent with the ring oxidation.[56–60] The first is the decrease in the Soret band intensity. Concomitantly, there are two new features increasing in intensity at 470 nm and 696 nm. The isosbestic points at 400 nm and 453 nm suggest the UV–vis spectra represent two species that are in equilibrium, which is consistent with the reversible nature of the CV results for **3**. Figure 2*b* shows the absorbance difference spectra of the data shown in Fig. 2*a*. The resulting plot shows more of the smaller transitions and clearly indicates isosbestic points as the data cross the $y = 0$ line. The growth of the largest peak at 470 nm is similar to other spectroelectrochemical results of other porphyrins and is tentatively assigned to the Soret band of the radical cation, **3**$^+$.

Fig. 2. Spectroelectrochemistry of **3**. (*a*) UV–vis spectra of compound **3** at an applied potential of +1.0 V. Each spectrum is recorded at 2 min intervals and arrows indicate the direction of peak change. (*b*) The absorbance difference spectra of the data shown in Fig. 2*a*. Positive peaks indicate peak growth compared with neutral porphyrin.

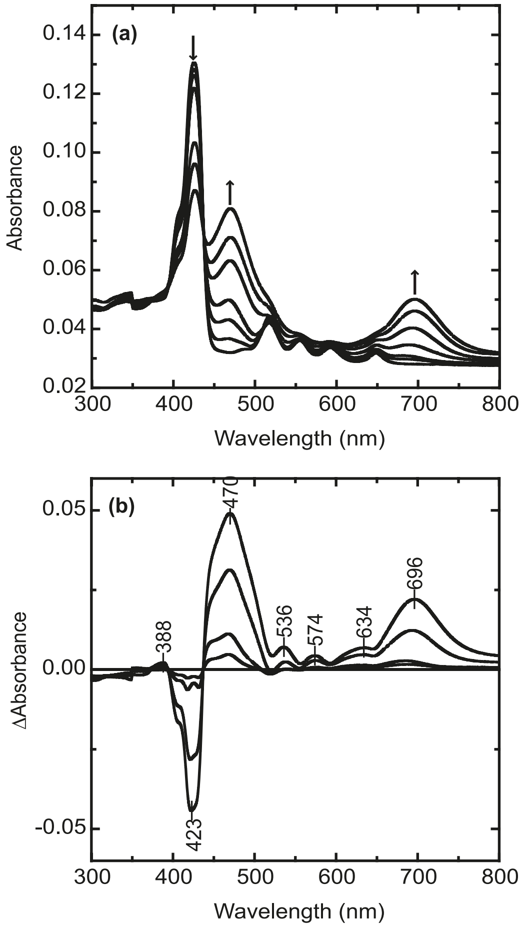

The smaller features that are visible in the difference spectra (Fig. 2*b*) at 536, 574, and 634 nm are assigned to the Q-bands of the oxidized porphyrin. After exhaustive oxidation of **3** to **3**$^+$, the potential was stepped to 1.2 V, where the conversion of **3**$^+$ to **3**$^{2+}$ is expected to occur. The absorption spectrum of **3**$^{2+}$ is not shown; however, no significant changes were observed with the exception of a slight increase in the peak at 696 nm. The lack of visible changes is due to two factors. First, the electronic transitions of **3**$^{2+}$

could be weak, and second, the cell design uses a longer path length (1 mm) such that the resultant spectrum is a linear combination of all three species diffusing into the light path. In addition, the oxidized form may be more reactive and decompose. Although CV evidence supports a stable redox couple, the spectroelectrochemical cell design does not permit exclusion of O_2 from the cell.

Spectroelectrochemical experiments were carried out with **4** to investigate the electronic structure of the oxidized form of **4**, which is included in the Supplementary data. The oxidation of **4** to **4**$^+$ shows a decrease in the Soret band with an applied potential of 0.8 V (first oxidation potential **4**/**4**$^+$). Upon oxidation, a new Soret band is seen evolving at 442 nm, which is blue-shifted from the **3**$^+$ radical cation species. New Q-bands of the radical cation (**4**$^+$) appear at 523, 577, 643, and 680 nm. In addition, a new broad transition occurs at 897 nm. Spectroelectrochemical experiments were also carried out at applied potentials equal to the second oxidation. However, at the $E_{1/2}^{\mathrm{ox}}(2)$, the spectral features were nearly the same as the spectrum of **4**$^+$. After spectral subtraction of the oxidized spectrum (**4**$^+$), a broad peak at ~900 nm was observed, but considering the long path length (1 mm), it is clear that the dication (**4**$^{2+}$) spectrum consists of neutral **4**, radical cation **4**$^+$, and the dication **4**$^{2+}$, which precludes accurate spectral deconvolution.

Structures **3**, **4**, **3**$^+$, **4**$^+$, **3**$^{2+}$, and **4**$^{2+}$ were energy optimized using DFT methods with the B3LYP basis set and 6-31+G functional using the Gaussian03 software package.[61] The summaries of the frontier orbital energy levels are shown in Fig. 3. Based on the gas-phase calculations, the HOMO energy levels of the free-base porphyrin **3** and the Zn-metalloporphyrin **4** are very similar in energy. This HOMO energy level trend was not observed in the experimentally determined oxidation potential. Experimental results show the Zn-porphyrin is easier to oxidize, suggesting it has a higher-lying HOMO. This inconsistency could arise from solvent effects that are not accounted for in the calculations. The two highest occupied FMOs of **3** and **4** are nearly degenerate and both have nearly degenerate LUMOs, consistent with the four-orbit model.[33] The HOMO–LUMO energy gap is similar for **3** and **4**, which is consistent with the observed electronic absorption spectroscopy. Both radical cations, **3**$^+$ and **4**$^+$, show red-shifted adsorptions compared with their neutral parent compounds. The SOMO of **4**$^+$ is nearly triply degenerate, whereas the SOMO of **3**$^+$ does not follow the same pattern. The FMOs of **3**$^+$ and **4**$^+$ are shown in Fig. 4. The triply degenerate occupied orbitals of **4**$^+$ are confined to the electron-rich trisalkoxy phenyl rings, in contrast to **3**$^+$, where the SOMO orbital is delocalized over the macrocyclic ring and the four trisalkoxy phenyl rings. The dication species **3**$^{2+}$ and **4**$^{2+}$ show the lowest HOMO–LUMO energy difference of 0.8 eV, corresponding to 1550 nm, which was not observed in the absorption spectra. In addition, the HOMOs of both dications are triply degenerate and the LUMOs are non-degenerate.

FMOs for all compounds are included in the Supplementary data. Starting with the neutral porphyrins **3** and **4**, the doubly degenerate HOMOs and LUMOs show electron density confined to the porphyrin macrocyclic ring. In addition, the energy-minimized structures have the meso-substituted phenyl rings perpendicular to the macrocyclic ring, implying little electronic perturbations can occur from a meso-phenyl substitution pattern. The monocations **3**$^+$ and **4**$^+$ have different minimized structures. The free base **3**$^+$ has a SOMO that is delocalized over the macrocyclic ring and the four phenyl meso-substituents and a twist in the meso-phenyl groups, such that contributions from the phenyl rings can participate in delocalization. In contrast, the Zn-porphyrin cation, **4**$^+$, maintains the same geometry as neutral **4** and the SOMO is limited to the four meso-substituted phenyl rings. Both LUMO and LUMO^{+1} of both monocations (**3**$^+$ and **4**$^+$) are centered on the macrocyclic ring system. The removal of an additional electron to the dications results in HOMOs that reside on the four phenyl substituents. In addition, both dications **3**$^{2+}$ and **4**$^{2+}$ show a twist in the meso-phenyl substituents allowing for stabilization of the dicationic macrocycle. The LUMOs of the dications show coefficients on both the phenyl substituents and the macrocycle. The calculations indicate extensive electronic tuning is possible by modifying the β-pyrrole positions, and limited HOMO energy level tun-

Fig. 3. DFT-calculated (B3LYP/6-31+G) energy levels of the frontier orbitals of the neutral, radical cation, and dication of compounds **3** and **4**. The HOMO–LUMO energy differences are shown over the arrows.

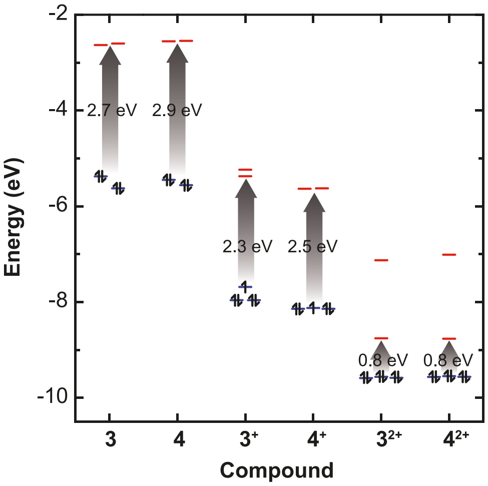

Fig. 4. FMOs of the radical cations **3**$^+$ and **4**$^+$ using DFT with the B3LYP basis set and 6-31G+ functional.

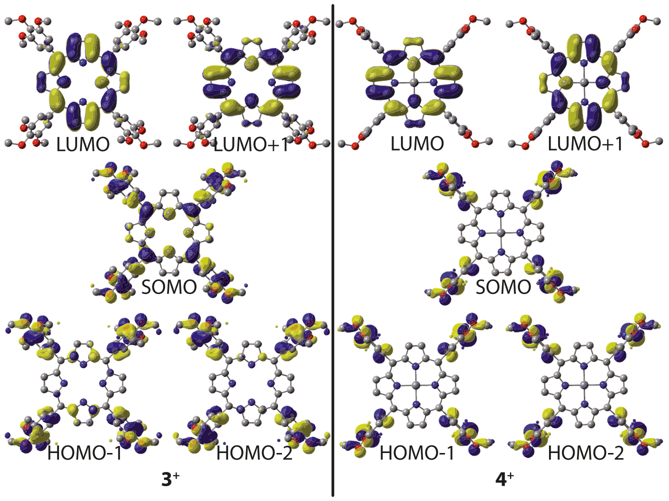

ing is possible using phenyl-substituted meso positions. However, the mono- and dications can be strongly stabilized by electron-rich meso-derivatives.

Conclusions

The optical measurements of the tetraarylporphyrins display typical behaviour with intense Soret and Q-band absorptions and fluorescence spectra with small Stokes shifts. Electrochemical oxidations of both the free-base porphyrin **3** and Zn-metalloporphyrin **4** show two reversible one-electron redox waves by cyclic voltammetry methods. Further analysis of the cyclic voltammetry data revealed an unusually large diffusion coefficient for **3**, suggesting aggregate formation. Considering the size and number of alkoxy groups, aggregation is feasible, as others have used such motifs to build long-range order in liquid crystals. The electron-transfer rate constants were 1.2×10^{-3} cm s^{-1} and 2.4×10^{-3} cm s^{-1} for compounds **3** and **4**, respectively, which falls within the range of other porphyrins. Spectroelectrochemical experiments suggest that the electron removed to form the radical cations ($\mathbf{3}^{+}$ and $\mathbf{4}^{+}$) is part of the porphyrin macrocycle. In addition, the spectroelectrochemical results are supported by the DFT-calculated energy-optimized structures of **3** and **4** in their neutral and radical cation states. The reversibility and stability of the oxidized forms of both **3** and **4** support the use of these compounds in organic devices as light harvesters or supramolecular charge-transfer assemblies. Of particular utility could be the excited-state energy of the oxidized porphyrin ring systems to generate charge-separated components used in solar energy conversion. The electrochemically determined HOMO energy levels of **3** and **4** are –5.3 eV and –5.1 eV (assuming the HOMO energy level of Fc/Fc^{+} is –4.8 eV), respectively, which is comparable to the ubiquitous poly-3-hexylthiophene (P3HT) at –5.0 eV and LUMO energy of –3.3 eV. The Rehm and Weller equation gives an estimate of LUMO energy levels of **3** and **4** at –3.4 eV and –3.1 eV, respectively, which is similar to P3HT. The similar energy levels of **3** and **4** with P3HT indicate porphyrins with their superior molar absorptivities could be used as alternative light-harvesting compounds (*p*-type material) in organic photovoltaic cells. In addition, the LUMO level of PCBM, at –3.7 eV, is lower than the excited-state energy of either **3** or **4**, allowing for a thermodynamic driving force for charge separation. Unfortunately, the tetraaryl substituents did not impart supramolecular properties, which would lead to organized structures that could carry charge more efficiently over long distances. Nevertheless, the electron-rich, trisalkoxy meso-substituted porphyrins are remarkably air and electrochemically stable, which is a design necessity for devices.

Supplementary data

Supplementary data for this article are available on the journal Web site (canjchem.nrc.ca).

Acknowledgements

The authors are grateful to the Natural Sciences and Engineering Research Council of Canada (NSERC), Alberta Government, Canadian Foundation for Innovation (CFI), and the Institute for Sustainable Energy, Environment and Economy, for funding.

References

(1) Wasielewski, M. R. *Chem. Rev.* **1992**, *92* (3), 435. doi:10.1021/cr00011a005.

(2) Gust, D.; Moore, T. A.; Moore, A. L. *Acc. Chem. Res.* **2001**, *34* (1), 40. doi:10.1021/ar9801301. PMID:11170355.

(3) Henderson, B. W.; Dougherty, T. J. *Photochem. Photobiol.* **1992**, *55* (1), 145. doi:10.1111/j.1751-1097.1992.tb04222.x. PMID:1603846.

(4) Meunier, B. *Chem. Rev.* **1992**, *92* (6), 1411. doi:10.1021/cr00014a008.

(5) Traylor, T. G.; Tsuchiya, S.; Byun, Y. S.; Kim, C. *J. Am. Chem. Soc.* **1993**, *115* (7), 2775. doi:10.1021/ja00060a027.

(6) Anson, F. C.; Shi, C. N.; Steiger, B. *Acc. Chem. Res.* **1997**, *30* (11), 437. doi:10.1021/ar960264j.

(7) Batinić-Haberle, I.; Spasojević, I.; Hambright, P.; Benov, L.; Crumbliss, A. L.; Fridovich, I. *Inorg. Chem.* **1999**, *38* (18), 4011. doi:10.1021/ic990118k.

(8) Wrighton, S. A.; Stevens, J. C. *Crit. Rev. Toxicol.* **1992**, *22* (1), 1. doi:10.3109/10408449209145319. PMID:1616599.

(9) Guengerich, F. P. *Annu. Rev. Pharmacol. Toxicol.* **1999**, *39* (1), 1. doi:10.1146/annurev.pharmtox.39.1.1. PMID:10331074.

(10) Sottocasa, G. L.; Kuylenstierna, B.; Ernster, L.; Bergstrand, A. *J. Cell Biol.* **1967**, *32* (2), 415. doi:10.1083/jcb.32.2.415. PMID:10976232.

(11) Ferrer-Sueta, G.; Hannibal, L.; Batinić-Haberle, I.; Radi, R. *Free Radic. Biol. Med.* **2006**, *41* (3), 503. doi:10.1016/j.freeradbiomed.2006.04.028.

(12) Wöhrle, D.; Meissner, D. *Adv. Mater.* **1991**, *3*, 129. doi:10.1002/adma.19910030303.

(13) Imahori, H.; Fukuzumi, S. *Adv. Funct. Mater.* **2004**, *14* (6), 525. doi:10.1002/adfm.200305172.

(14) Lane, P. A.; Palilis, L. C.; O'Brien, D. F.; Giebeler, C.; Cadby, A. J.; Lidzey, D. G.; Campbell, A. J.; Blau, W.; Bradley, D. D. C. *Phys. Rev. B Condens. Matter* **2001**, 63.

(15) Grinstaff, M. W.; Hill, M. G.; Labinger, J. A.; Gray, H. B. *Science* **1994**, *264* (5163), 1311. doi:10.1126/science.8191283. PMID:8191283.

(16) Bhyrappa, P.; Young, J. K.; Moore, J. S.; Suslick, K. S. *J. Am. Chem. Soc.* **1996**, *118* (24), 5708. doi:10.1021/ja953474k.

(17) Bock, C. R.; Connor, J. A.; Gutierrez, A. R.; Meyer, T. J.; Whitten, D. G.; Sullivan, B. P.; Nagle, J. K. *J. Am. Chem. Soc.* **1979**, *101* (17), 4815. doi:10.1021/ja00511a007.

(18) Balzani, V.; Juris, A.; Venturi, M.; Campagna, S.; Serroni, S. *Chem. Rev.* **1996**, *96* (2), 759. doi:10.1021/cr941154y. PMID:11848772.

(19) Guldi, D. M.; Prato, M. *Acc. Chem. Res.* **2000**, *33* (10), 695. doi:10.1021/ar990144m. PMID:11041834.

(20) Dolphin, D.; Felton, R. H. *Acc. Chem. Res.* **1974**, *7* (1), 26. doi:10.1021/ar50073a005.

(21) Roberts, J. E.; Hoffman, B. M.; Rutter, R.; Hager, L. P. *J. Biol. Chem.* **1981**, *256* (5), 2118. PMID:6257699.

(22) Erman, J. E.; Vitello, L. B.; Mauro, J. M.; Kraut, J. *Biochemistry* **1989**, *28* (20), 7992. doi:10.1021/bi00446a004. PMID:2557891.

(23) Ravikanth, M.; Chandrashekar, T. K. Nonplanar Porphyrins and Their Biological Relevance: Ground and Excited-State Dynamics. In *Coordination Chemistry;* 1995; Vol. 82, pp 105–188.

(24) Kadish, K. M.; Lin, M.; van Caemelbecke, E.; De Stefano, G.; Medforth, C. J.; Nurco, D. J.; Nelson, N. Y.; Krattinger, B.; Muzzi, C. M.; Jaquinod, L.; Xu, Y.; Shyr, D. C.; Smith, K. M.; Shelnutt, J. A. *Inorg. Chem.* **2002**, *41* (25), 6673. doi:10.1021/ic0200702. PMID:12470062.

(25) Meier, H.; Müller, K. *Angew. Chem. Int. Ed. Engl.* **1995**, *34* (1314), 1437. doi:10.1002/anie.199514371.

(26) Pieterse, K.; Lauritsen, A.; Schenning, A. P. H. J.; Vekemans, J. A. J. M.; Meijer, E. W. *Chem. Eur. J.* **2003**, *9* (22), 5597. doi:10.1002/chem.200305073.

(27) Tanabe, K.; Yasuda, T.; Yoshio, M.; Kato, T. *Org. Lett.* **2007**, *9* (21), 4271. doi:10.1021/ol701741e. PMID:17887690.

(28) Terazzi, E.; Torelli, S.; Bernardinelli, G.; Rivera, J.-P.; Bénech, J.-M.; Bourgogne, C.; Donnio, B.; Guillon, D.; Imbert, D.; Bünzli, J. C.; Pinto, A.; Jeannerat, D.; Piguet, C. *J. Am. Chem. Soc.* **2005**, *127* (3), 888. doi:10.1021/ja0446101. PMID:15656627.

(29) van Gorp, J. J.; Vekemans, J. A. J. M.; Meijer, E. W. *J. Am. Chem. Soc.* **2002**, *124* (49), 14759. doi:10.1021/ja020984n. PMID:12465989.

(30) Wang, D. H.; Shen, Z.; Guo, M.; Cheng, S. Z. D.; Harris, F. W. *Macromolecules* **2007**, *40* (4), 889. doi:10.1021/ma061763v.

(31) Cheng, F.; Adronov, A. *Chem. Eur. J.* **2006**, *12* (19), 5053. doi:10.1002/chem.200600302.

(32) Nowak-Król, A.; Gryko, D.; Gryko, D. T. *Chem. Asian J.* **2010**, *5* (4), 904. doi:10.1002/asia.200900693. PMID:20235275.

(33) Gouterman, M. *J. Mol. Spectrosc.* **1961**, *6*, 138. doi:10.1016/0022-2852(61)90236-3.

(34) Gouterman, M. In *The Porphyrins;* Dolphin, D., Ed.; Academic Press: New York, 1978; Vol. 3, pp 1–165.

(35) Giraudeau, A.; Callot, H. J.; Gross, M. *Inorg. Chem.* **1979**, *18* (1), 201. doi:10.1021/ic50191a042.

(36) Renner, M. W.; Barkigia, K. M.; Zhang, Y.; Medforth, C. J.; Smith, K. M.; Fajer, J. *J. Am. Chem. Soc.* **1994**, *116* (19), 8582. doi:10.1021/ja00098a019.

(37) Ghosh, A. *J. Am. Chem. Soc.* **1995**, *117* (16), 4691. doi:10.1021/ja00121a025.

(38) Woller, E. K.; DiMagno, S. G. *J. Org. Chem.* **1997**, *62* (6), 1588. doi:10.1021/jo962159t.

(39) Guilard, R.; Kadish, K. M. *Chem. Rev.* **1988**, *88* (7), 1121. doi:10.1021/cr00089a007.

(40) Kadish, K. M.; Vancaemelbecke, E.; Boulas, P.; Dsouza, F.; Vogel, E.; Kisters, M.; Medforth, C. J.; Smith, K. M. *Inorg. Chem.* **1993**, *32* (20), 4177. doi:10.1021/ic00072a005.

(41) Gregg, B. A.; Fox, M. A.; Bard, A. J. *J. Am. Chem. Soc.* **1989**, *111* (8), 3024. doi:10.1021/ja00190a041.

(42) Gregg, B. A.; Fox, M. A.; Bard, A. J. *J. Phys. Chem.* **1990**, *94* (4), 1586. doi:10.1021/j100367a068.

(43) Schouten, P. G.; Warman, J. M.; de Haas, M. P.; Fox, M. A.; Pan, H.-L. *Nature* **1991**, *353* (6346), 736. doi:10.1038/353736a0.

(44) van der Boom, T.; Hayes, R. T.; Zhao, Y. Y.; Bushard, P. J.; Weiss, E. A.; Wasielewski, M. R. *J. Am. Chem. Soc.* **2002**, *124* (32), 9582. doi:10.1021/ja026286k. PMID:12167053.

(45) Fleming, B. D.; Bond, A. M. *Electrochim. Acta* **2009**, *54* (10), 2713. doi:10.1016/j.electacta.2008.11.042.

(46) Kampas, F. J.; Yamashita, K.; Fajer, J. *Nature* **1980**, *284* (5751), 40. doi:10.1038/284040a0.

(47) Bedioui, F.; Devynck, J.; Bied-Charreton, C. *Acc. Chem. Res.* **1995**, *28* (1), 30. doi:10.1021/ar00049a005.

(48) Malinski, T.; Ciszewski, A.; Bennett, J.; Fish, J. R.; Czuchajowski, L. *J. Electrochem. Soc.* **1991**, *138* (7), 2008. doi:10.1149/1.2085915.

(49) Bard, A. J.; Faulkner, L. R. *Electrochemical Methods: Fundamentals and Applications,* 2nd ed.; Wiley: New York, 2001; p xxi, 833 p.

(50) Nicholson, R. S. *Anal. Chem.* **1965**, *37* (11), 1351. doi:10.1021/ac60230a016.

(51) Kadish, K. M.; Davis, D. G. *Ann. N. Y. Acad. Sci.* **1973**, *206* (1 The Chemical), 495. doi:10.1111/j.1749-6632.1973.tb43232.x. PMID:4518403.

(52) Kuo, M. C.; Li, L. A.; Yen, W. N.; Lo, S. S.; Lee, C. W.; Yeh, C. Y. *Dalton Trans.* **2007**, (14): 1433. doi:10.1039/b617170b. PMID:17387405.

(53) Rehm, D.; Weller, A. *Ber. Bunsen-Ges.* **1969**, *73*, 834.

(54) Rehm, D.; Weller, A. *Isr. J. Chem.* **1970**, *8*, 259.

(55) Pandian, R. P.; Chandrashekar, T. K.; Saini, G. S. S.; Verma, A. L. *J. Chem. Soc., Faraday Trans.* **1993**, *89* (4), 677. doi:10.1039/ft9938900677.

(56) El-Kasmi, A.; Lexa, D.; Maillard, P.; Momenteau, M.; Saveant, J. M. *J. Am. Chem. Soc.* **1991**, *113* (5), 1586. doi:10.1021/ja00005a022.

(57) Langhus, D. L.; Wilson, G. S. *Anal. Chem.* **1979**, *51* (8), 1139. doi:10.1021/ac50044a012.

(58) Kadish, K. M.; Mu, X. *Pure Appl. Chem.* **1990**, *62* (6), 1051. doi:10.1351/pac199062061051.

(59) Lin, C.-.; Fang, M.-Y.; Cheng, S.-H. *J. Electroanal. Chem.* **2002**, *531* (2), 155. doi:10.1016/S0022-0728(02)01056-2.

(60) Sooambar, C.; Troiani, V.; Bruno, C.; Marcaccio, M.; Paolucci, F.; Listorti, A.; Belbakra, A.; Armaroli, N.; Magistrato, A.; De Zorzi, R.; Geremia, S.; Bonifazi, D. *Org. Biomol. Chem.* **2009**, *7* (11), 2402. doi:10.1039/b820210a. PMID:19462051.

(61) Frisch, M. J.; Trucks, G. W.; Schlegel, H. B.; Scuseria, G. E.; Robb, M. A.; Cheeseman, J. R.; Montgomery, J. A., Jr.; Vreven, T.; Kudin, K. N.; Burant, J. C.; Millam, J. M.; Iyengar, S. S.; Tomasi, J.; Barone, V.; Mennucci, B.; Cossi, M.; Scalmani, G.; Rega, N.; Petersson, G. A.; Nakatsuji, H.; Hada, M.; Ehara, M.; Toyota, K.; Fukuda, R.; Hasegawa, J.; Ishida, M.; Nakajima, T.; Honda, Y.; Kitao, O.; Nakai, H.; Klene, M.; Li, X.; Knox, J. E.; Hratchian, H. P.; Cross, J. B.; Bakken, V.; Adamo, C.; Jaramillo, J.; Gomperts, R.; Stratmann, R. E.; Yazyev, O.; Austin, A. J.; Cammi, R.; Pomelli, C.; Ochterski, J. W.; Ayala, P. Y.; Morokuma, K.; Voth, G. A.; Salvador, P.; Dannenberg, J. J.; Zakrzewski, V. G.; Dapprich, S.; Daniels, A. D.; Strain, M. C.; Farkas, O.; Malick, D. K.; Rabuck, A. D.; Raghavachari, K.; Foresman, J. B.; Ortiz, J. V.; Cui, Q.; Baboul, A. G.; Clifford, S.; Cioslowski, J.; Stefanov, B. B.; Liu, G.; Liashenko, A.; Piskorz, P.; Komaromi, I.; Martin, R. L.; Fox, D. J.; Keith, T.; Al-Laham, M. A.; Peng, C. Y.; Nanayakkara, A.; Challacombe, M.; Gill, P. M. W.; Johnson, B.; Chen, W.; Wong, M. W.; Gonzalez, C.; Pople, J. A. *Gaussian 03,* Revision E.01; Gaussian, Inc.: Wallingford, CT, 2004.